EAST EUROPEAN JOURNAL OF PHYSICS. 3. 413-417 (2025)
DOI:10.26565/2312-4334-2025-3-43 ISSN 2312-4334

GROWTH OF $BaZrS_3$ CHALCOGENIDE PEROVSKITE THIN FILMS WITHOUT POST-ANNEALING

T.M. Razykov[a,b], K.M. Kuchkarov[a,b], R.T. Yuldoshov[a,b]*, M.P. Pirimmatov[a], R.R. Khurramov[a], D.Z. Isakov[a], M.A. Makhmudov[a,b], S.A. Muzafarova[b], A. Matmuratov[a]
[a]*Physical-Technical Institute, Chingiz Aytmatov Street 2B, Tashkent 100084, Uzbekistan*
[b]*Institute of Semiconductors Physics and Microelectronics, Yangi Olmazor Street 20, Tashkent 100057, Uzbekistan*
**Corresponding Author, E-mail: ruhiddin@yahoo.com*
Received April 24, 2025; revised August 8, 2025; accepted August 21, 2025

Tandem solar cells based on hybrid organic–inorganic metal halide perovskites have achieved power conversion efficiencies of up to 28%. However, issues related to long-term stability and lead (Pb) toxicity have prompted the search for earth-abundant, chemically stable, and non-toxic alternatives. In this work, we report the first vacuum evaporation synthesis of $BaZrS_3$ (barium zirconium sulfide) thin films at a substrate temperature of 550 °C. The resulting films exhibit near-stoichiometric Ba:Zr ratios and strong light absorption, with absorption coefficients exceeding 10^5 cm^{-1} near 1.9 eV. Under controlled conditions, a baseline oxygen content of 4–6% was consistently observed. The absence of an additional sulfurization step markedly increased the resistance of the thin film and suppressed the dark current by approximately three orders of magnitude, indicating a substantial reduction in carrier density likely resulting from a decreased concentration of sulfur vacancies. These findings highlight the potential of $BaZrS_3$ as a stable, lead-free absorber for next-generation photovoltaics.
Keywords: *$BaZrS_3$; Chalcogenide perovskites; Energy-dispersive X-ray spectroscopy; Optical bandgap; Photo-response*
PACS: 73.61. Le

INTRODUCTION

Chalcogenide perovskites have recently gained significant research interest as promising lead-free, inorganic perovskite semiconductors. Compared to hybrid halide perovskites like $CH_3NH_3PbI_3$, chalcogenide perovskites exhibit significantly improved structural stability. Most conventional semiconductors are covalent materials characterized by four-fold coordination of both cations and anions. However, in the past decade, organic-inorganic halide perovskites have emerged as competitive alternatives for photovoltaic applications, challenging traditional semiconductors in unprecedented ways. These perovskites are ionic materials with higher coordination, which enhances the Coulomb attraction between cations and anions. Their strong ionicity is believed to reduce the formation of deep-level anti-site defects that contribute to non-radiative carrier recombination.

Unlike conventional semiconductors, halide perovskites exhibit unusually low carrier concentrations (~10^{13}/cm^3) and extremely long carrier lifetimes (on the order of 1 μs) [1]. The power conversion efficiency (PCE) of solar cells based on halide perovskites has seen a dramatic increase, from an initial 3.8% in 2009 to over 25% in 2019 [2]. Perovskites refer to a class of crystalline compounds with the general formula ABX_3, where the B-site cation has six nearest-neighbor anions (X), and the A-site cation occupies a cavity formed by eight corner-sharing BX_6 octahedra (Figure 1).

The most extensively studied perovskites are complex metal oxides, where X is oxygen. These oxides are technologically significant due to their multifunctionality and tunable properties. Conventional semiconductors and oxide/halide perovskites represent two extremes in the spectrum of covalency and ionicity. Covalent bonding is directional, making electronic and optical properties sensitive to bond distortions, whereas ionic bonding is associated with strong electron correlation due to reduced dielectric screening. Achieving a balance between ionicity and covalency opens pathways to discovering novel semiconductors with enhanced properties. Despite their potential, only limited efforts have been devoted to developing materials that bridge the gap between these bonding characteristics. Recently, chalcogenide perovskites have emerged as a novel class of semiconductors, where sulfur (S) or selenium (Se) replaces oxygen as the anion. Compared to oxide perovskites, chalcogenide perovskites exhibit reduced band gaps, making them well-suited for visible and near-infrared (NIR) light applications. Among these, $BaZrS_3$ (barium zirconium sulfide) has attracted attention due to its promising optoelectronic properties, initially predicted through theoretical studies. These properties include band gap values suitable for photovoltaics, an exceptionally high absorption coefficient, tolerance to deep defects, strong dielectric screening, favorable phonon characteristics, and isotropic electron mobility for efficient charge transport. [3-11]

Additionally, $BaZrS_3$ is composed of earth-abundant and non-toxic elements [12, 13]. Although $BaZrS_3$ and related chalcogenide perovskites were synthesized over half a century ago, they have received minimal attention until recently. After extensive theoretical screening, several ABX_3 chalcogenide materials have been identified as potential candidates

Cite as: T.M. Razykov, K.M. Kuchkarov, R.T. Yuldoshov, M.P. Pirimmatov, R.R. Khurramov, D.Z. Isakov, M.A. Makhmudov, S.A. Muzafarova, A. Matmuraov, East Eur. J. Phys. 3, 413 (2025), https://doi.org/10.26565/2312-4334-2025-3-43

for photovoltaic applications. These materials exhibit strong light absorption and direct bandgap optical transitions, making them very promising for high-performance optoelectronic devices. Notably, $BaZrS_3$ was confirmed to have a distorted perovskite structure with a band gap of approximately 1.7 eV and strong light absorption, aligning well with theoretical predictions [14]. This material has demonstrated exceptional stability against pressure, moisture, and oxidation, with minimal degradation even four years post-synthesis. However, due to the current lack of high-quality thin films, many fundamental properties of chalcogenide perovskites remain unexplored, posing a challenge to their broader implementation in optoelectronics.

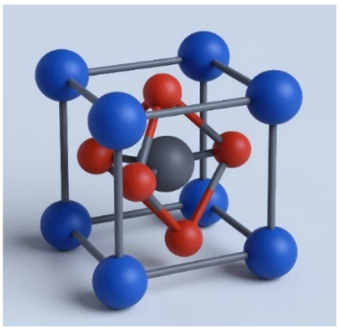

Figure 1. Crystal structures of $BaZrS_3$. exhibit distorted perovskite structures.
Blue spheres: A-site cations (e.g., Ba^{2+} or Ca^{2+}), positioned at the corners. Gray sphere: B-site cation (e.g., Ti^{4+}, Zr^{4+}), in the center. Red spheres: anions (O, S^{2-}), at the face centers

EXPERIMENTAL PART

$BaCl_2$ (Barium chloride) (20.800 g, 100 mmol) was first dispersed in 200 mL of deionized water. Subsequently, 5.0 N H_2SO_4 (Sulfuric acid) (33.3 mL, 100 mmol) was slowly added to the dispersion under vigorous stirring while maintaining the reaction mixture in an ice bath [15].

The reaction between $BaCl_2$, H_2SO_4, and water (H_2O) leads to the formation of barium sulfate ($BaSO_4$) and hydrochloric acid (HCl):

$$BaCl_2+H_2SO_4 \rightarrow BaSO_4\downarrow+2HCl \quad (1)$$

$BaSO_4$ is insoluble in water and precipitates out as a white solid. HCl (Hydrochloric acid) remains in solution. This is a double displacement reaction (precipitation reaction), where the sulfate ion (SO_4^{2-}) from sulfuric acid displaces the chloride ions from barium chloride, forming the insoluble $BaSO_4$ precipitate. Since H_2O is already present in the reaction medium (if aqueous solutions are used), it does not directly participate in the reaction but serves as medium for the ions to react.

The reaction was terminated after 5 hours, and $BaSO_4$ was recovered via centrifugation. The obtained product was subsequently washed with deionized water three times before being dried in an oven at 110 °C overnight. BaS was synthesized by reducing $BaSO_4$, using a 25% hydrogen-balanced argon atmosphere by chemical molecular beam deposition (CMBD) system at 1000 °C for 1 hour [16]. The resulting BaS product appeared as a white powder, which was immediately transferred into a nitrogen-filled glovebox and finely ground into a homogeneous powder.

A mixture of BaS (7.407 g, 43.732 mmol) and elemental sulfur (S) (2.804 g, 87.46 mmol) was prepared by grinding with an agate mortar and pestle inside the glovebox. The homogenized mixture was then placed into a pre-dried borosilicate glass tube, which was subsequently flame-sealed under vacuum to form an ampule. The ampule was heated in a muffle furnace from room temperature to 400 °C and maintained at this temperature for 12 hours. The furnace was then turned off, allowing the sample to cool to room temperature gradually. BaS_3 and ZrS_2 powders were placed in two separate molybdenum boats under a high-vacuum environment of 10^{-5}-10^{-6} mmHg. The reaction was conducted for 1,5 hours at a substrate temperature of 550 °C. (Figure 2).

Figure 2. Photographic image of the BaS_3 and ZrS_2 in vacuum chamber

The surface morphology of the thin films was characterized using a JSM-IT510 (JEOL) scanning electron microscope (SEM) operating in secondary electron mode at an accelerating voltage of 20 kV. Elemental composition was analyzed via Energy Dispersive X-ray (EDX) spectroscopy using an Aztec Energy Advanced Spectrometer, which offers an energy resolution of 127 eV and a detection sensitivity of 0.5 wt.%. Optical absorption spectra were recorded at room temperature using a Shimadzu UV-1900i UV–Vis–NIR spectrophotometer. Current–voltage (I–V) characteristics were recorded using a Keithley 2460 source meter under AM1.5G simulated sunlight (1600 W xenon lamp, Model No. UHE-NL-250, Sciencetech, Canada).

RESULTS AND DISCUSSIONS

Scanning electron microscopy was employed to examine the morphological characteristics of the $BaZrS_3$ thin films, while energy-dispersive X-ray spectroscopy was used to verify their elemental composition. The analysis revealed a clear correlation between substrate temperature and the microstructural evolution of the films. Morphology of samples presented in Figure 3 indicates that higher substrate temperatures enhance grain growth and favor the formation of rod-shaped $BaZrS_3$ grains aligned parallel to the substrate surface. Notably, the sample fabricated at 550 °C exhibited grains exceeding 0.5-1 µm in size, with a uniform distribution across the substrate, indicative of a homogeneous and well-controlled growth process.

The observed increase in grain size with temperature is attributed to enhanced atomic diffusion and coalescence phenomena during the film deposition process, which collectively contribute to improved crystallinity and preferential grain orientation. Although $BaZrS_3$ films have shown continuity with thicknesses ranging from 350 nm. The rusults of EDX analysis, as shown in Figure 4 approximately 4% oxygen was detected in the bulk of $BaZrS_3$ film, with a nearly stoichiometric Ba:Zr composition. Despite efforts to minimize the duration of air exposure prior to measurement, the precursors consistently retained a baseline oxygen content of at least 4-5%, a value that remained unchanged even after several weeks of storage in this environment.

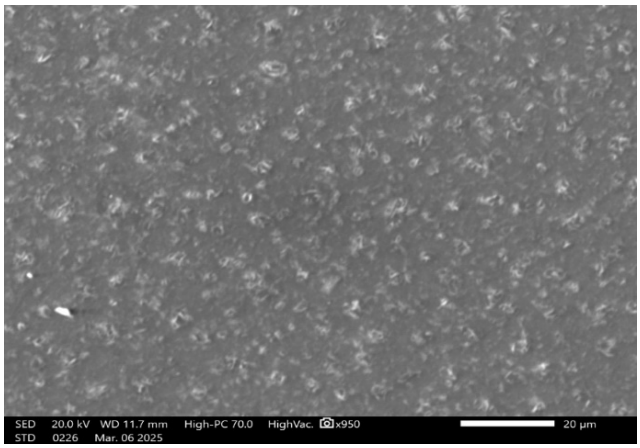

Figure 3. SEM top views of the $BaZrS_3$ thin films obtained 550 °C substrate temperature

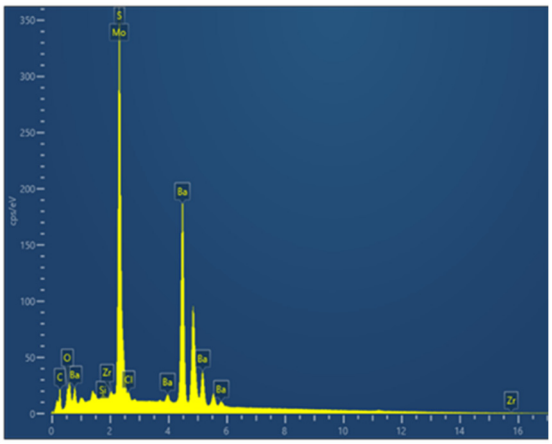

Figure 4. Typical EDX spectra of synthesized $BaZrS_3$ thin films

In various experimental trials, an increase in oxygen concentration was only observed after annealing the samples, with the oxygen content rising by up to 10%. (These conclusions will be given in detail in subsequent works). This reaction appears to be linked to the presence of excess sulfur in the samples. The precursors were slightly sulfur-rich, and oxidation was notably enhanced when excess sulfur vapor was introduced during the annealing process. During the thermal process, $BaZrS_3$ crystallizes from the precursor and some of the sulfur-rich material is reduced by sulfur gas evaporation (S(g)), leading to removal of sulfur without oxidation. However, it has been suggested that the stresses generated within the films during this process, which predispose them to oxidation, may contribute to the formation of holes.

The band gaps of $BaZrS_3$ with distorted perovskite structure have been theoretically calculated to be around 1.7-1.85 eV and have also been experimentally verified to be within the same range [16].

Figure 5 presents the UV-Vis absorption spectrum of the $BaZrS_3$ thin film deposited at a substrate temperature of 550 °C, plotted as a function of photon energy. The film's geometry enabled the calculation of the absorption coefficient (α). A significant increase in α is observed around 1.9 eV, surpassing 10^5 cm^{-1}, indicating the strong light absorption capability of $BaZrS_3$. Assuming a direct allowed electronic transition, the optical band gap energy (Eg) was determined using the Tauc relation:

$$(\alpha h\nu)^2 = A(h\nu - E_g) \quad (2)$$

where $h\nu$ is the photon energy, A is a material-dependent constant, and α is the absorption coefficient. The band gap energy was estimated by extrapolating the linear region of the $(\alpha h\nu)^2$ versus $h\nu$ plot to the photon energy axis. Based on this method, the $BaZrS_3$ thin film exhibited a direct optical band gap of approximately 1.9 eV

The I-V curves under both dark and illuminated conditions are presented in Figure 6. However, the sulfurization process was not performed to enhance the photo-response. This decision was made to avoid potential degradation from prolonged high-temperature exposure, which could induce sulfur vacancies and increase carrier concentration. Indicating a substantial decrease in carrier density due to sulfur vacancies, As shown in Figure 6, the absence of sulfurization significantly increases the junction resistance and reduces the dark current by approximately three orders of magnitude, Nevertheless, the photo-response is notably enhanced. These findings highlight the importance of suppressing dark current by further reducing carrier concentration to achieve optimal photodetector performance. To address sulfur vacancies, we propose high-pressure sulfurization as a strategy. Prolonged high-temperature treatment induces the formation of sulfur vacancies, resulting in an increased carrier concentration

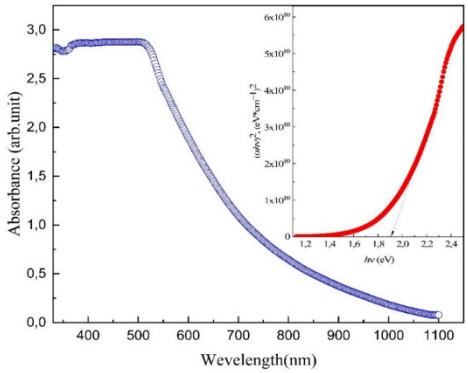

Figure 5. Absorbance for $BaZrS_3$ thin films and Tauc plots $BaZrS_3$ thin films

Notably, no additional sulfurization was conducted to further enhance the photo-response. This approach is justified by the high sulfur content in the precursor, as well as the lower substrate temperature employed compared to conventional chalcogenide perovskite layer fabrication methods, which significantly reduce sulfur re-evaporation from the substrate surface. To further enhance performance, we propose that methods such as p-type doping or sulfurization under high-pressure conditions could be utilized. These methods can help passivate sulfur vacancy states, thereby reducing their negative impact on device performance. As shown in figure 6, eliminating the sulfurization without results in a significant increase in the sample resistivity, accompanied by a substantial reduction in the dark current by three orders of magnitude. This observation suggests a marked decrease in the carrier density, which is likely attributed to the reduction in sulfur vacancies. Therefore, these results imply that to achieve improved photodetector performance, it is essential to suppress dark current by effectively reducing the carrier concentration.

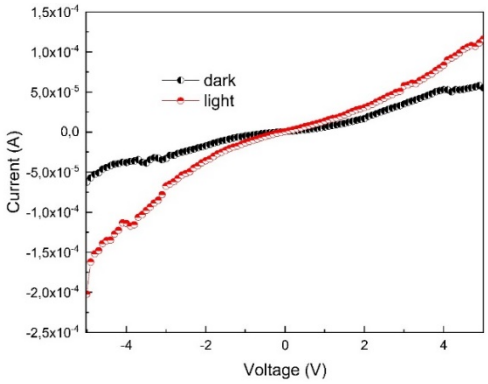

Figure 6. The I-V curves in the dark and under illumination

CONCLUSION

The successful development of a BaS_3 extraction technique, combined with co-deposition of BaS_3 and ZrS_2 powders under high vacuum, enabled controlled synthesis conditions. As a result, $BaZrS_3$ thin films with an optical bandgap of 1.9 eV and absorption coefficients exceeding 10^5 cm^{-1} was successfully fabricated. The elimination of an additional sulfurization step led to a significant increase in film resistivity and a ~1000-fold reduction in dark current. This behavior indicates a notable decrease in free carrier concentration, which is likely due to the suppression of sulfur vacancies - common donor-like defects in chalcogenide semiconductors. These findings highlight the critical role of defect management in optimizing the optoelectronic properties of $BaZrS_3$-based devices.

Acknowledgements

This work was supported by the Basic Research Program of the Academy of Sciences of the Republic of Uzbekistan, Ministry of innovative development of the Republic of Uzbekistan (Grant № FL-8824063282).

ORCID

Takhirdjon. M. Razykov, https://orcid.org/0000-0001-9738-3308; **Kudrat M. Kuchkarov,** https://orcid.org/0000-0002-2238-7205; **Ruhiddin T. Yuldoshov,** https://orcid.org/0000-0002-7886-1607; **Muhammad M. Pirimmatov,** https://orcid.org/0009-0000-4829-7817; **Ramozan R. Khurramov,** https://orcid.org/0009-0008-1038-0138; **Diyorbek Z. Isakov,** https://orcid.org/0000-0003-4314-5683; **Sultanpasha A. Muzafarova,** https://orcid.org/0000-0001-5491-7699; **Aydos Matmuratov**, https://orcid.org/0009-0005-6121-6424

REFERENCES

[1] D.W. de Quilettes, S.M. Vorpahl, S.D. Stranks, H. Nagaoka, G.E. Eperon, M.E. Ziffer, H.J. Snaith, and D.S. Ginger, "Impact of microstructure on local carrier lifetime in perovskite solar cells," Science, **348**, 683-686 (2015). https://doi.org/10.1126/science.aaa5333

[2] S. Suragtkhuu, S. Sunderiya, P. Myagmarsereejid, S. Purevdorj, A.S.R. Bati, B. Bold, *et al*., "Graphene-Like Monoelemental 2D Materials for Perovskite Solar Cells," Adv. Energy Mater. **13**, 2204074 (2023). https://doi.org/10.1002/aenm.202204074

[3] A. Swarnkar, W.J. Mir, R. Chakraborty, M. Jagadeeswararao, T. Sheikh, A. Nag, "Are Chalcogenide Perovskites an Emerging Class of Semiconductors for Optoelectronic Properties and Solar Cell?" Chem. Mater. **31**, 565−575 (2019). https://doi.org/10.1021/acs.chemmater.8b04178

[4] K.V. Sopiha, C. Comparotto, J.A. Márquez, and J.J.S. Scragg, "Chalcogenide Perovskites: Tantalizing Prospects, Challenging Materials," Advanced Optical Materials, **10**, 2101704 (2022). https://doi.org/10.1002/adom.202101704

[5] M. Buffiere, D.S. Dhawale, and F. El-Mellouhi, "Chalcogenide Materials and Derivatives for Photovoltaic Applications," Energy Technology, **7**, 1900819 (2019). https://doi.org/10.1002/ente.201900819

[6] C. Comparotto, P. Ström, O. Donzel-Gargand, T. Kubart, and J.J.S. Scragg, "Synthesis of BaZrS3 Perovskite Thin Films at a Moderate Temperature on Conductive Substrates," ACS Appl. Energy Mater. **5**(5), 6335–6343 (2022). https://doi.org/10.1021/acsaem.2c00704

[7] C. Wang, R. Nie, Y. Dai, H. Tai, B. Zhu, L. Zhao, Y. Wu, *et al*., "Enhancing the inherent stability of perovskite solar cells through chalcogenide-halide combinations," Energy Environ. Sci. **17**, 1368-1386 (2024). https://doi.org/10.1039/D3EE03612J

[8] R. Jaramillo, and J. Ravichandran, "In praise and in search of highly- polarizable semiconductors: Technological promise and discovery strategiesm," APL Materials, **7**, 100902 (2019). https://doi.org/10.1063/1.5124795

[9] Y. Nishigaki, T. Nagai, M. Nishiwaki, T. Aizawa, M. Kozawa, K. Hanzawa, Y. Kato, *et al*., "Extraordinary Strong Band-Edge Absorption in Distorted Chalcogenide Perovskites," Solar RRL, **4**, 1900555 (2020). https://doi.org/10.1002/solr.201900555

[10] X. Wu, W. Gao, J. Chai, C. Ming, M. Chen, H. Zeng, P. Zhang, *et al*., "Defect tolerance in chalcogenide perovskite photovoltaic material $BaZrS_3$," Science China Materials, **64**, 2976−2986 (2021). https://doi.org/10.1007/s40843-021-1683-0

[11] W. Meng, B. Saparov, F. Hong, J. Wang, D.B. Mitzi, and Y. Yan, "Alloying and Defect Control within Chalcogenide Perovskites for Optimized Photovoltaic Application," Chem. Mater. **28**, 821-829 (2016). https://doi.org/10.1021/acs.chemmater.5b04213

[12] M. Ishii, and M. Saeki, "Raman and Infrared Spectra of BaTiS3 and BaNbS3," Phys. Stat. Sol. (b), **170**, K49 (1992). https://doi.org/10.1002/pssb.2221700149

[13] M. Ishii, M. Saeki, and M. Sekita, "Vibrational spectra of barium-zirconium sulfides," Mater. Res. Bull. **28**, 493-500 (1993). https://doi.org/10.1016/0025-5408(93)90132-W

[14] S. Perera, H. Hui, C. Zhao, H. Xue, F. Sun, C. Deng, N. Gross, *et al*., "Chalcogenide perovskites – an emerging class of ionic semiconductors," Nano Energy, **22**, 129-135 (2016). https://doi.org/10.1016/j.nanoen.2016.02.020

[15] R. Yang, J. Nelson, C. Fai, H.A. Yetkin, C. Werner, M. Tervil, A.D. Jess, *et al*., "A Low-Temperature Growth Mechanism for Chalcogenide Perovskites," Chemistry of Materials, **35**(12), 4743–4750 (2023). https://doi.org/10.1021/acs.chemmater.3c00494

[16] T.M. Razykov, K.M. Kuchkarov, B.A. Ergashev, L. Schmidt-Mende, T. Mayer, M. Tivanov, M. Makhmudov, *et al*., "Growth and characterization of $Sb_2(S_xSe_{1-x})_3$ thin flms prepared by chemical-molecular beam deposition for solar cell applications," Thin Solid Films, **807**, 140554 (2024). https://doi.org/10.1016/j.tsf.2024.140554

[17] S. Agarwal, K.C. Vincent, and R. Agrawal, "From synthesis to application: a review of $BaZrS_3$chalcogenide perovskites," Nanoscale, **17**, 4250-4300 (2025). https://doi.org/10.1039/D4NR03880K

ВИРОЩУВАННЯ ТОНКІХ ПЛІВОК ХАЛЬКОГЕНІД ПЕРОВСКІТУ $BaZrS_3$ БЕЗ НАСТУПНОГО ВІДПАЛЮВАННЯ

Т.М. Разиков[a,b], К.М. Кучкаров[a,b], Р.Т. Юлдошов[a,b], М.П. Пірімматов[a], Р.Р. Хуррамов[a], Д.З. Ісаков[a], М.А. Махмудов[a,b], С.А. Музафарова[b], А. Матмуратов[a]

[1] Фізико-технічний інститут, вул. Чингіза Айтматова 2Б, Ташкент 100084, Узбекистан

[2] Інститут фізики напівпровідників і мікроелектроніки, вул. Янгі Олмазор, 20, Ташкент 100057, Узбекистан

Тандемні сонячні батареї на основі гібридних органіко-неорганічних галогенідів металів перовскітів досягли ефективності перетворення електроенергії до 28%.) Однак проблеми, пов'язані з довгостроковою стабільністю та токсичністю свинцю (Pb), спонукали до пошуку поширених у землі, хімічно стабільних і нетоксичних альтернатив. У цій роботі ми повідомляємо про перший синтез тонких плівок $BaZrS_3$ (сульфіду барію і цирконію) методом вакуумного випаровування при температурі підкладки 550 °C. Отримані плівки демонструють майже стехіометричне співвідношення Ba:Zr і сильне поглинання світла з коефіцієнтами поглинання, що перевищують 10^5 $см^{-1}$ поблизу 1,9 еВ. (У) контрольованих умовах стабільно спостерігався вихідний вміст кисню 4–6%. Відсутність додаткової стадії сульфування помітно збільшила опір тонкої плівки та придушила темновий струм приблизно на три порядки величини, що вказує на суттєве зменшення щільності носія, ймовірно, внаслідок зниження концентрації вакансій сірки. Ці висновки підкреслюють потенціал $BaZrS_3$ як стабільного безсвинцевого поглинача для фотоелектричних пристроїв нового покоління.

Ключові слова: *$BaZrS_3$; халькогенідні перовскіти; енергодисперсійна рентгенівська спектроскопія; оптична заборонена зона; фотовідгук*